THE LONG-LIVED FUSOGENIC STATE INDUCED IN ERYTHROCYTE GHOSTS BY ELECTRIC PULSES IS NOT LATERALLY MOBILE

ARTHUR E. SOWERS
Jerome H. Holland Laboratory for the Biomedical Sciences, American Red Cross, Rockville, Maryland 20855

ABSTRACT The long-lived fusogenic state induced in spherical-shaped erythrocyte ghosts by electric field pulses (Sowers, A.E. 1984. *J. Cell Biol.* 99:1989–1996; Sowers, A.E. 1986. *J. Cell Biol.* 102:1358–1362) was studied in terms of how the fusion yield depended on both (*a*) the location where membrane–membrane contact took place with respect to the orientation of the electric pulse and (*b*) the time interval between the pulse treatment and membrane–membrane contact. Fusion yields were greater for membrane–membrane contact locations closer to where the pulse-induced transmembrane voltage was expected to be greatest and showed a time interval–dependent accelerating decay. The portion of the membrane that became fusogenic included the area up to a latitude of ~ 38° of arc towards the equators of the membranes. A time interval–dependent increase or decrease in rate of decay in the fusion yield for membrane–membrane contacts induced closer to the equator of the membranes did not occur showing that the pulse-induced fusogenic state is immobile in the early 5–45-s interval after induction and has a rate of decay, which does not permit long time interval changes in lateral position to be measured.

INTRODUCTION

Electrically induced membrane fusion (electrofusion) has five unique characteristics that are useful in studying membrane fusion mechanisms (for reviews see references 1–4). They are: (*a*) the potential for very high fusion yields, (*b*) high fusion synchrony, (*c*) the possibility for time coordination of fusion events with other devices, (*d*) delivery of the fusion stimulus independent of exogenous chemicals, and (*e*) the electrically inducible fusogenic membrane alteration in erythrocyte ghosts (5–7) and some other membrane systems (3) is long-lived. Electrofusion has also been successfully used in numerous applications and found in several cases to be the method of choice (1–3). For example, real-time studies on single cells are also practical (8). In addition, in two freeze fracture electron microscopy studies both the application of fusion-initiating pulses and the moment that the samples were quick frozen were time-coordinated and showed fusion-relevant ultrastructural details (9, 10).

The usual electrofusion protocol calls first for the induction of membrane–membrane contact by dielectrophoretically aligning the membranes into the so-called pearl-chain formation (1–3, 11). This is done by using a chamber with two electrodes that conduct a constant amplitude but low strength alternating electric current through the membrane suspension. Fusion is then induced while the membranes are in contact when a high strength direct current (DC) pulse is applied to the same electrodes. While the amplitudes, directions, and duration of the two electric field treatments will be different, the use of the same two electrodes causes the axis of the field lines to be identical. The significant aspect of this is that dielectrophoresis induces membrane–membrane contact at the same two points in spherical-shaped membranes which, according to theory (12–15), experience the highest electric field-induced transmembrane voltage during the pulse. These two points are commonly referred to as the "poles." The same theory predicts that the transmembrane voltage will always be zero at the "equator" of the membranes.

From our discovery that fusion can occur in human erythrocyte ghosts even if membrane–membrane contact is induced after the pulse treatment we concluded that a long-lived fusogenic alteration was induced in the membrane (5–7). Since the fusogenic stimulus (the pulses) induces a property (the fusogenic state) that cannot be measured unless a second condition is induced (membrane–membrane contract), we refer to the induced property in terms of its "fusogenicity." The above observation led to the question of how the fusion yields would change if membrane–membrane contact were induced at various times after the pulse but at points other than at the poles of the erythrocyte ghosts. We answered this question by using a special chamber with four electrodes arranged in a square (Figs. 1 and 2). Two of the electrodes were used to apply the pulses with one field direction then all four were used to induce an alternating electric field in a different

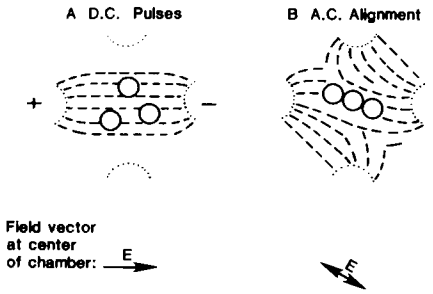

FIGURE 1 Example of protocol for measurement of fusogenicity as a function of location of membrane–membrane contact as a function of distance from poles of membrane (see text). (*a*) Pulse treatment of membrane suspension with membranes in random positions, (*b*) alignment of membranes into a pearl chain alignment direction, which is different from the electric field direction generated by direct current pulses. Note the location of electrode ports (*dotted lines*) and that the electric field lines (*dashed lines*) are only approximate.

direction. The angles between the two directions could be reproducibly and precisely controlled by external electrical circuitry. This paper is a report of these experiments. Portions of these results have appeared in preliminary form (16).

METHODS

Concepts

Human erythrocyte ghost membranes become dielectrophoretically aligned into pearl chains that are oriented parallel to the electric field direction in sodium phosphate buffer (pH 8.5) up to 60 mM in strength. They do not exhibit spinning or rotation (for review see reference 17) along any axis if 60 Hz alternating current is used (4, 6, 7). Since electric fields are vector fields, the electric field direction can be calculated from the vector sum of the components for any chamber/electrode/medium combination (18). Thus the pearl-chain alignment direction can be different than the field direction from the pulse if appropriate alignment voltages are applied at all four electrodes.

Membranes

The preparation and labeling of human erythrocyte ghost membranes with the fluorescent lipid analogue 1,1'-dihexadecyl-3,3,3',3'-tetramethylindocarbocyanine perchlorate (DiI) were as previously described (6, 7). The erythrocytes were hemolyzed, and the ghosts were washed in sodium phosphate buffer (20 mM, pH 8.5) and stored overnight in that buffer as a pellet. The next day the pellet was resuspended in sodium phosphate buffer (60 mM, pH 8.5), pelleted, and then resuspended in the same buffer to the desired membrane concentration. All operations were performed at 0°–4°C. The fusion assay was conducted at 20°–22°C.

Apparatus

The electrical circuit used to supply the alignment-inducing alternating current and the fusion-inducing pulses was described previously (6). A special four-electrode chamber (Fig. 2) and associated circuit (Fig. 3) permitted the alternating current carried by the four electrodes to be varied in such a way that the direction of the resultant alternating electric field at the center of the chamber could be changed with respect to the direction of the pulsed electric field. This circuit was connected between the alternating current source, the pulse generator, and the four electrodes of the chamber and permitted the passage of direct current

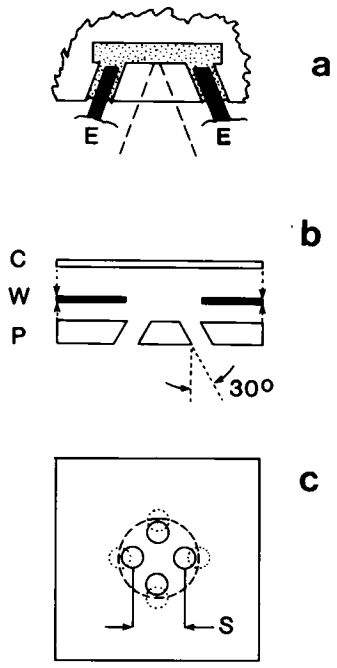

FIGURE 2 Cylindrical-shaped four-electrode chamber with low height-to-radius ratio used for inducing close membrane–membrane contact at locations other than poles: (*a*) chamber in cross-section (plane of paper is parallel to axis of microscope light path). Convergent light from phase condenser shown by dashed lines. Electrodes, *E*, are No. 22 gauge tinned solid copper wire. Membrane suspension (*dotted area*) fills all of available volume; (*b*) chamber is constructed by heat sealing a standard microscope coverslip, *C*, to a 2.4-mm thick Plexiglas (Rohm and Hass, West Hill, Ontario, Canada) sheet, *P*, with a 0.127-mm thick Parafilm (American Can Co., Greenwich, CT) washer, *W*, with hole 5.5 mm in diameter. Wells for electrodes (1.6-mm diam) are holes drilled at angle of 30° of arc with plane of plastic to permit phase condenser light to illuminate the membrane suspension; (*c*) view of Plexiglass sheet from microscope objective lens. Holes intersect with plane of plastic block at surface closest to microscope objective (*solid circles*) and at plane of surface closest to phase condenser (*dotted circles*). Holes are in corners of a square with centers in opposite corners spaced S = 3.2 mm. Center of hole in plastic washer (*dashed line*) is concentric with center of four wells. Assembled chamber is carried by frame as shown in Fig. 1 of reference 6.

pulses through only two electrodes. Various predetermined proportions of the constant amplitude sine wave voltage could be applied for alignment simultaneously to each of all four electrodes (Figs. 1 and 5).

Using simplifying assumptions it can be shown that for switch positions 1–5 of the circuit in Fig. 3 the resultant field direction at the center of the chamber should have angles of θ = 59°, 53°, 45°, 38°, and 30° of arc with respect to the direct current pulse direction. Actual alignment angles measured from micrographs of ten dielectrophoretically aligned ghost-membrane pearl chains located at or very close to the center of the chamber averaged: θ = 69°, 38°, 27°, 18°, and 12° of arc, respectively. The average standard deviation was 3° of arc. The deviations from theory were due to variabilities in electrode wire position in electrode wells, machining tolerance in electrode well position and angle, and uneven sealing and alignment of the center of the Parafilm washer within the center point equidistant from the centers of the four electrode wells. Actual alignments, however, were reproducible and therefore suitable for the qualitative results sought.

Protocol

A suspension of membranes was placed into the chamber through one of the four ports using a syringe carrying a short blunt-tipped hypodermic needle. Membranes were treated by applying eight DC pulses (1,400 V peak) to the two electrodes as shown in Fig. 1. The pulses had an exponentially decaying waveform with decay half-time of 0.8 ms and were applied at the rate of 2/s. The membranes were then aligned into contact after intervals of 5, 45, or 85 s. Taking the effective distance between each electrode as 2.4 mm (Fig. 2) each pulse therefore generated a field strength of ~ 583 V/mm in the center of the fusion chamber. Membrane alignment was induced by turning on the 60-Hz alternating voltage of 20–25 V (rms) at the input of the circuit in Fig. 3 and leaving it

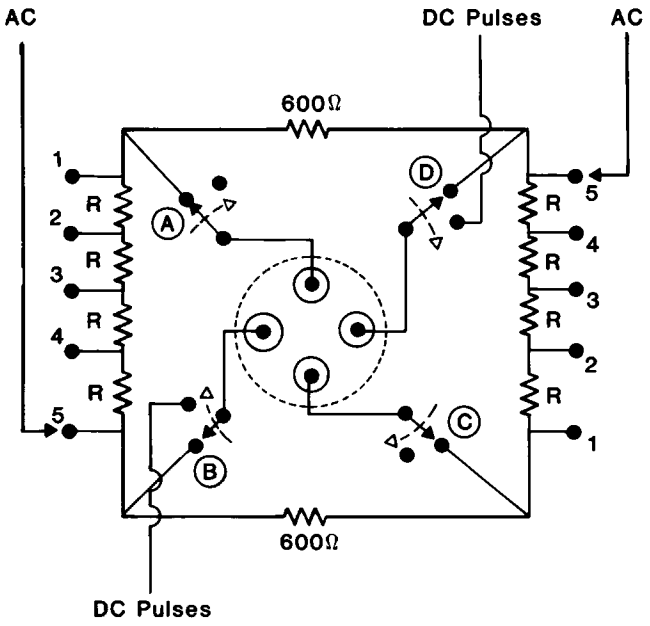

FIGURE 3 Circuit for providing alternating current and one set of constant alternating current to four electrodes for variable angle dielectrophoresis. Chamber (circumference, *dashed circle*) containing electrode holes and electrodes (*open circles* concentric with *solid circles*) connected with arms (*solid arrows*) of four associated relays *A–D*, shown in normally closed position. Activation of these relays (*dotted arrows*) connects electrodes associated with relays *B* and *D* to the pulse generator and disconnects electrodes associated with relays *A* and *C*. Two ganged switches connect alternating current to junctions (*arrows* and *numbered dots*) of four sets of fixed resistors (R = 100 Ω) in a bridge with two 600 Ω resistors. Alternating current is from the secondary of a step down transformer connected to the utility lines through a variable voltage autoformer. Pulses are from generator as previously described (Fig. 1 of reference 6).

on. After alignment all fusion events were counted. Fusion events were revealed as membrane–membrane contact took place and fluorescence moved from a labeled membrane to at least one originally unlabeled membrane in a pearl chain containing a mixture (14:1, in numbers) of unlabeled and DiI-labeled membranes. Fusion yield, in percent, was calculated by dividing the number of fusion events by the sum of (*a*) the number of originally labeled but unfused membranes plus (*b*) the number of fusion events in the same sample field of view, and multiplying by 100. After fusion events were scored, the alternating voltage was turned off and the chamber was extensively flushed with buffer and then refilled with a fresh suspension of membranes.

Heat generation by the two electrical treatments was previously shown by the absence of melting in low melting temperature waxes to be low or insignificant (6, 7). As previously described, these membranes changed shape upon pulse treatment (6) and the discoid shape became spherical. Since some net membrane translational movement is induced electrophoretically upon pulse application and mechanically by Brownian motion, a fraction of all pulse-treated membranes touch each other before membrane–membrane contact was induced by dielectrophoresis. This resulted in a background fusion yield which was determined to be 2.5% from separate experiments by counting fusion events after the application of the same pulses but without subsequent application of the alternating current to induce membrane–membrane contact. This background fusion yield was subtracted from gross fusion yields to give net fusion yield. The worst case average standard deviation was 1.3 absolute percentage units (Fig. 4).

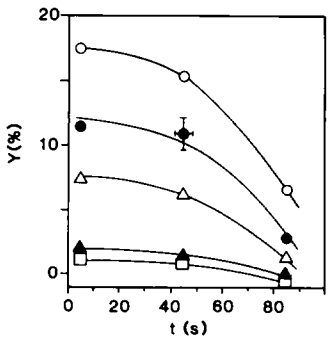

FIGURE 4 Net fusion yield (Y) obtained upon membrane contact as a function of time interval (t) between pulse treatment and dielectrophoretically induced membrane–membrane contact. Off-pole membrane–membrane contact locations are: (○) 12°; (●) 18°; (△) 27°; (▲) 38°; and (□) 69°. Note that net fusion yield at 69° for a time interval of 85 s is negative (see text). Worst case (for 12° contact location) error bars are one standard deviation each side of the mean.

RESULTS

Regardless of where membrane–membrane contact was induced with respect to the poles, net fusion yields exhibited a decay that accelerated with time (Fig. 4). The net fusion yields were higher if membrane–membrane contact was induced at points closer to the poles (Fig. 5). Net fusion yields for membrane–membrane contact at points θ = 38° and 69° of arc from the poles were no more than 2% regardless of the time interval between the pulse treatment and induced membrane–membrane contact and reflect scatter in the data. Lines drawn through net fusion yield measurements for θ = 12°, 18°, 27°, and 38° contact locations for 5- and 45-s time interval data and a line drawn through the net fusion yield measurement for the 12° and 18° contact locations for the 85-s data were straight and parallel, or nearly so, to one another. Net fusion yields remained at or below 2% for membrane contact at points nearer the equator (38° and 69° of arc from the poles) regardless of the interval between the pulse treatment and the induction of membrane–membrane contact. Net fusion yields for the 45- and 85-s time interval data were normalized to the net fusion yield at the 12°

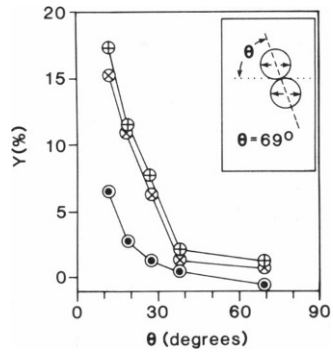

FIGURE 5 Net fusion yield (Y) observed upon membrane–membrane contact at off-pole contact locations (see Fig. 4 legend). Averages of measured angles between pulse field and alignment field are given in degrees. (*b*) Fusion yield as a function of alignment angles shown in *a* and time interval between pulse treatment and close membrane–membrane contact: (⊕) 5 s; (⊗) 45 s; (⊙) 85 s. (*Inset*) Example alignment showing relationship between poles (*arrows*) on membranes receiving maximum transmembrane induced voltage from the pulse electric field treatment (direct current pulse direction indicated by dotted line) followed by the dielectrophresis-induced alignment direction (*dashed lines*) from the alternating current passing through all four electrodes. Angle, θ, between axis (*dotted line*) and membrane–membrane contact axis (*dashed line*).

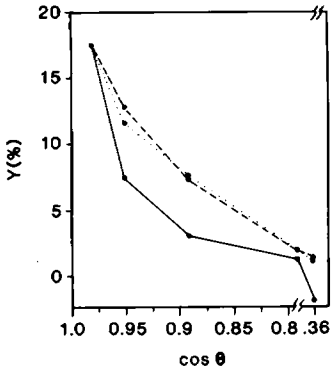

FIGURE 6 Net fusion yield (Y) obtained upon membrane–membrane contact at off-pole contact locations and plotted against $\cos\theta$. All 45 s (*dotted*) and 85 s (*solid*) data from Fig. 5 are normalized to net fusion yield measured for the 5 s (*dashed*) time interval at the 12° contact location (see Fig. 4 legend).

contact location for the 5-s time interval and plotted as a function of $\cos\theta$ and shown in Fig. 6.

DISCUSSION

The same four-electrode chamber was used in a previous study to make a preliminary determination of the location on the membrane of the induced fusogenic state and its change in location with time (7). In that study membrane–membrane contact was induced at only two points (the poles and the equator) and showed that (*a*) only the poles became fusogenic, and (*b*) the fusion yield for contact at the equator never rose above the background for any time interval between the pulse treatment and the induction of membrane–membrane contact. Hence it was concluded that while the fusogenic membrane alternation was induced in the same part of the membrane which experienced the highest induced transmembrane voltages, the long-lived fusogenic state was otherwise laterally immobile. However, it was also possible (*a*) that relocation of the fusogenic property to the equators by lateral diffusion was too slow to be detected by those experiments, (*b*) that the pulse-induced fusogenic membrane alteration needed to be above a threshold for fusion events to occur, or (*c*) that the fusogenic state decayed more quickly compared with how far it could diffuse laterally. In the present study the induced fusogenicity was measured at five points of membrane contact instead of only two in the previous study (7). Furthermore these locations were between the poles and the equators of these membranes and represented a study with substantially greater lateral resolution. Compared with net fusion yields for membrane–membrane contact locations closer to the poles, any detectable lateral diffusion of fusogenic sites or time-dependent relocation of the fusogenic membrane alteration away from the poles should have increased with time interval or decreased more slowly (i.e., a time-dependent decrease in slope) at locations farther from the poles compared with locations closer to the poles (i.e., a general time-dependent broadening of the width of the curve should be observable). Thus the slopes of the lines through the first four points for both the 5-and the 45-s time intervals and the first two points for the 85-s interval in Fig. 5 should have decreased markedly with time or the fusogenicity-location relationship should have shown a wave that propagated towards the equator. As such all of these lines were parallel to one another within experimental error. That the 5- and 45-s data can be superposed within experimental error suggests that in the early time intervals after induction but before decay processes dominate, the slopes are identical. When the 45- and 85-s interval data were replotted normalized to the net fusion yield at the 12° contact location for the 5-s interval and against $\cos\theta$, the curve showed no time-dependent broadening (Fig. 6). In fact the slight narrowing in the curve for the 85-s time interval for the $\cos\theta = 0.98$ and 0.95 contact locations suggests that 85 s after the induction of the long-lived fusogenic state and accelerating decay overtakes any broadening that would have occurred. A hint of slight curve broadening, however, may be present between the $\cos\theta = 0.95$ and 0.89 points and also between the $\cos\theta = 0.89$ and 0.79 points in the 85-s interval and may be partly due to tumbling, which would be expected to begin to show up after such an interval. This indicates that in the early time interval (5–45 s) after the pulse treatment essentially no lateral movement of the fusogenic alteration is detectable. After larger time intervals (85 s) between the pulse treatment and induced membrane–membrane contact lateral movement, if it exists, is swamped by other processes (decay and tumbling).

That the plot of normalized net fusion yields against $\cos\theta$ (Fig. 6) is relatively linear for the 5- and 45-s time interval data are consistent with the well known (1–3, 12–15, 17, 21) and simplified relationship between induced membrane voltage, V, at a location angle, θ (specified in Fig. 5) bulk external electric field, E, and radius of spherical membrane, r, as given by the equation $V = 1.5\ Er\cos\theta$. Exact correspondence is obtained if a constant, C, representing the threshold transmembrane voltage needed to induce the fusogenic alteration, is added to the right side of this equation (This assumes a one-to-one relationship between V and Y when $V > C$). Such a threshold is consistent with what is known about electrofusion (1–4). Also, that both the net fusion yield and the induced membrane potential have the same cosine dependence suggests that the important factor is, indeed, the component of the electric field, which is perpendicular to the membrane plane and not the bulk electric field.

The time-dependent acceleration in the decay in the fusogenic state may be due to interactions between different populations of pulse-induced membrane alterations, one of which is fusogenic. The fusogenic population of altered structure could be a decay product of an unstable but nonfusogenic alteration. In connection with this possibility, a recently published study of electrofusion showed ultrastructural evidence for multiple classes of pulse-induced structures with different lifetimes (9).

Our results have implications for the mechanism of membrane electrofusion (for reviews see 1–4). So far only one mechanism has been hypothesized for electrofusion

(19, 20). In this hypothesis the pulses induce cylindrical pores (electropores) in each of the two close-spaced membranes. Each electropore in one membrane is concentrically paired with an identical electropore in the other membrane. Fusion of the two membranes then occurs as the edges of the two electropores reseal with each other instead of themselves. Depending on experimental conditions electropores may reseal very quickly or very slowly after formation (for reviews see references 4, 15, 21,22).

As previously presented (1–4), the electropore hypothesis applies, however, only to the protocol in which close membrane–membrane contact is established before and maintained during the application of the fusion-inducing pulses. In this respect, the original form of the electropore hypothesis does not predict the long-lived fusogenic state. However, in a modification of the electropore hypothesis it may be possible that preformed pores (i.e., long-lived residual electropores) in membranes in suspension could collide head-on or edge-to-edge with each other to bring free edges of pores together as the membranes are aligned into contact. Thus the electropores can be thought of as fusogenic sites as well as parts of intermediate structures in the fusion event (for review see reference 4). However, results of two other studies (7, 22) suggest that the electropore hypothesis is unlikely to explain the long-lived fusogenic state on the grounds that total pore cross-sectional area of residual electropores, as a fraction of the total membrane area, may be far lower than needed to account for the observed fusion yields.

If electropores are the fusogenic sites and are made entirely of lipids as previously proposed (1–4, 19–20) then they should be laterally mobile and should diffuse in the plane of the membrane at rates comparable with other mobile membrane components because diffusion of a laterally mobile membrane component in a fluid membrane should be relatively independent of its effective diameter (23, 24) and it should not matter whether the entity is a solid (protein or lipid) or a hole filled with the aqueous medium. Thus fusion yields at some location away from the poles should have either increased measureably with time or decreased more slowly depending on the electropore lifetime compared with the rate of lateral diffusion. Although Brownian motion-induced tumbling can result in disorientation of fusogenic areas the experimental data indicate this was not enough to disorient the membranes and broaden the width of the fusogenicity-location curve (Fig. 6) except for contact locations where net fusion yields are so low as to be near the experimental scatter in the data.

The new data in the present paper show that if the long-lived fusogenic structural alteration appears to diffuse laterally in the plane of the membrane then during its lifetime it diffuses at a rate that is exceptionally low or is immobile. Our present understanding of membranes indicates that a fraction of many membrane proteins are laterally immobile (for reviews see references 25–27). Our observation suggests that the fusogenic membrane alteration may be somehow linked to the erythrocyte cytoskeletal system. This in turn casts doubt on the concept of a fusogenic electropore as being exclusively composed of lipids.

The expert technical assistance of Ms. Veena Kapoor is greatly appreciated.

This work is contribution No. 727 from the American Red Cross and was supported by Office of Naval Research contract N00014-87-K-0199.

Received for publication 28 October 1986 and in final form 17 August 1987.

Note Added in Proof: The long-lived fusogenic state has also been reported in Chinese hamster ovary cells (Teissie, J., and M. P. Rols. 1986. *Biochem. Biophys. Res. Commun.* 140:258–266).

REFERENCES

1. Zimmerman, U. 1982. Electric field-mediated fusion and related electrical phenomena. *Biochim. Biophys. Acta.* 694:227–277.
2. Zimmerman, U., J. Vienken, J. Halfmann, and C. C. Emeis. 1985. Electrofusion: a novel hybridization technique. *In* Advances in Biotechnological Processes. Vol. IV. A. Mizrah and A. L. van Wezel, editors. Alan R. Liss Inc., New York. 79–150.
3. Bates, G., J. Saunders, and A. Sowers. 1987. Electrofusion: principles and applications. *In* Cell Fusion. A. E. Sowers, editor. Plenum Publishing Corp., New York. 367–395.
4. Sowers, A. E., and V. Kapoor. 1987. The electrofusion mechanism in erythrocyte ghosts. *In* Cell Fusion. A. E. Sowers, editor. Plenum Publishing Corp., New York. 397–408.
5. Sowers, A. E. 1983. Red cell and red cell membrane shape changes accompanying the application of electric fields for inducing fusion. *J. Cell Biol.* 97(5, Pt. 2):178*a*. (Abstr.)
6. Sowers, A. E. 1984. Characterization of electric field induced fusion in erythrocyte ghost membranes. *J. Cell Biol.* 99:1989–1996.
7. Sowers, A. E. 1986. A long-lived fusogenic state is induced in erythrocyte ghosts by electric pulses. *J. Cell Biol.* 102:1358–1362.
8. Sowers, A. E. 1985. Movement of a fluorescent lipid label from a labeled erythrocyte membrane to an unlabeled erythrocyte membrane following electric field induced fusion. *Biophys. J.* 47:519–525.
9. Stenger, D. A., and S.-W. Hui. 1986. Kinetics of ultrastructural changes during electrically-induced fusion of human erythrocytes. *J. Membr. Biol.* 93:43–53.
10. Sowers, A. E. 1983. Fusion of mitochondrial inner membranes by electric fields produces inside out vesicles: visualization by freeze-fracture electron microscopy. *Biochim. Biophys. Acta.* 735:426–428.
11. Pohl, H. A. 1978. Dielectrophoresis. Cambridge University Press, London. 579 pp.
12. Neumann, E., and K. Rosenheck. 1973. Potential difference across vesicular membranes. *J. Membr. Biol.* 14:193–196.
13. Neumann, E., M. Schaefer-Ridder, Y. Wang, and P. H. Hofschneider. 1982. Gene transfer into mouse lyoma cells by electroporation in high electric fields. *EMBO (Eur. Mol. Biol. Organ.) J.* 1:841–845.
14. Teissie, J., and T. Y. Tsong. 1981. Electric field induced transient pores in phospholipid vesicles. *Biochemistry.* 20:1548–1554.
15. Tsong, T. Y. 1983. Voltage modulation of membrane permeability and energy utilization in cells. *Biosci. Rep.* 3:487–505.
16. Sowers, A. E. 1986. Long-lived fusogenic membrane sites induced by electric field pulses are not free to diffuse laterally in plane of the membrane. *Biophys. J.* 49:132a. (Abstr.)

17. Arnold, W. M., and U. Zimmerman. 1984. Electric field-induced fusion and rotation of cells. *Biol. Membr.* 5:389–454.
18. Reitz, J. R., and F. J. Milford. 1967. Foundations of Electromagnetic Theory. Addison-Wesley Publishing Co. Inc. Reading, MA. 25–27.
19. Pilwat, G., H.-P. Richter, and U. Zimmerman. 1981. Giant culture cells by electric field-induced fusion. *FEBS (Fed. Eur. Biochem. Soc.) Lett.* 133:169–174.
20. Dimitrov, D. S., and R. K. Jain. 1984. Membrane stability. *Biochim. Biophys. Acta.* 779:437–468.
21. Knight, D. E., and M. C. Scrutton. 1986. Gaining access to the cytosol: the technique and some applications of electropermeabilization. *Biochem. J.* 234:497–506.
22. Sowers, A. E., and M. R. Lieber. 1986. Electropore diameters, lifetimes, numbers, and locations in individual erythrocyte ghosts. *FEBS (Fed. Eur. Biochem. Soc.) Lett.* 205:179–184.
23. Saffman, P. G., and M. Delbruck. 1975. Brownian motion in biological membranes. *Proc. Natl. Acad. Sci. USA.* 72:3111–3113.
24. Peters, R., and R. J. Cherry. 1982. Lateral and rotational diffusion of bacteriorhodopsin in lipid bilayers: experimental test of the Saffman-Delbruck equations. *Proc. Natl. Acad. Sci. USA.* 79:4317–4321.
25. Peters, R. 1981. Translational diffusion in the plasma membrane of single cells as studied by fluorescence microphotolysis. *Cell Biol. Int. Rep.* 5:733–760.
26. Cherry, R. J. 1979. Rotational and lateral diffusion of membrane proteins. *Biochim. Biophys. Acta.* 559:289–327.
27. Peterson, N. O. 1984. Diffusion and aggregation in biological membranes. *Can. J. Biochem.* 62:1158–1166.